Monthly Notices of the ROYAL ASTRONOMICAL SOCIETY

MNRAS **511,** L35–L39 (2022) https://doi.org/10.1093/mnrasl/slab126
Advance Access publication 2021 December 14

What does lie at the Milky Way centre? Insights from the S2-star orbit precession

C. R. Argüelles,[1,2,3★] M. F. Mestre,[1,4] E. A. Becerra-Vergara,[2,3,5★] V. Crespi,[1] A. Krut,[2,3] J. A. Rueda[2,3,6,7★] and R. Ruffini[2,3,6,7]

[1]*Facultad de Ciencias Astronómicas y Geofísicas, Universidad Nacional de La Plata, Paseo del Bosque, B1900FWA La Plata, Argentina*
[2]*ICRANet, Piazza della Repubblica 10, I-65122 Pescara, Italy*
[3]*ICRA, Dipartimento di Fisica, Sapienza Università di Roma, P.le Aldo Moro 5, I-00185 Rome, Italy*
[4]*Instituto de Astrofísica de La Plata, UNLP & CONICET, Paseo del Bosque, B1900FWA La Plata, Argentina*
[5]*GIRG, Escuela de Física, Universidad Industrial de Santander, Bucaramanga 680002, Colombia*
[6]*ICRANet-Ferrara, Dipartimento di Fisica e Scienze della Terra, Università degli Studi di Ferrara, Via Saragat 1, I-44122 Ferrara, Italy*
[7]*INAF, Istituto de Astrofisica e Planetologia Spaziali, Via Fosso del Cavaliere 100, I-00133 Rome, Italy*

Accepted 2021 November 30. Received 2021 November 29; in original form 2021 September 10

ABSTRACT

It has been recently demonstrated that both, a classical Schwarzschild black hole (BH), and a dense concentration of self-gravitating fermionic dark matter (DM) placed at the Galaxy centre, can explain the precise astrometric data (positions and radial velocities) of the S-stars orbiting Sgr A∗. This result encompasses the 17 best resolved S-stars, and includes the test of general relativistic effects such as the gravitational redshift in the S2-star. In addition, the DM model features another remarkable result: The dense core of fermions is the central region of a continuous density distribution of DM whose diluted halo explains the Galactic rotation curve. In this Letter, we complement the above findings by analysing in both models the relativistic periapsis precession of the S2-star orbit. While the Schwarzschild BH scenario predicts a unique prograde precession for S2, in the DM scenario, it can be either retrograde or prograde, depending on the amount of DM mass enclosed within the S2 orbit, which, in turn, is a function of the DM fermion mass. We show that all the current and publicly available data of S2 cannot discriminate between the two models, but upcoming S2 astrometry close to next apocentre passage could potentially establish if Sgr A∗ is governed by a classical BH or by a quantum DM system.

Key words: stars: kinematics and dynamics – Galaxy: centre – Galaxy: structure – dark matter.

1 INTRODUCTION

The most effective method to explore the nature of the supermassive compact object at the centre of our Galaxy, Sgr A∗, has been the tracing of the orbits of the S-cluster stars. This astrometric data acquisition has been performed by two leading groups, one of which started a significant progress in constraining the central object mass (Eckart & Genzel 1997; Schödel et al. 2002; Gillessen et al. 2009, 2017; Genzel et al. 2010). More recently, this group has incorporated the GRAVITY instrument of the VLT, allowing us to detect the gravitational redshift of the S2-star (Gravity Collaboration et al. 2018a), to detect flares or hotspots close to Sgr A∗ (Gravity Collaboration et al. 2018b), and to detect the relativistic precession of the S2-star orbit of about 12 arcmin cycle^{-1} as predicted by the Schwarzschild BH (Gravity Collaboration et al. 2020). In parallel, a second group reached similar constraints to the mass of the central compact object in Sgr A∗ (Ghez et al. 1998, 2005, 2008; Boehle et al. 2016), mainly operating with the Keck, Gemini North, and Subaru Telescopes, using the Adaptative Optics technique. This group has recently confirmed the detection of the S2-star relativistic redshift (Do et al. 2019), converging with the first group in an estimate of the central object mass of about $4 \times 10^6\,M_\odot$.

From these two observational campaigns, the inference on the nature of Sgr A∗ has been reached on the ground of novel theoretical understandings. A recent important result has been obtained in Matsumoto, Chan & Piran (2020) (see also Tursunov et al. 2020), by re-considering the flare emissions around Sgr A∗, emphasizing both, that their motion is not purely geodesic, and establishing a limit on the spin of a putative Kerr BH mass of $|a| < 0.5$. Soon after, in Becerra-Vergara et al. (2020), it was introduced an alternative model to the classical BH in Sgr A∗ by re-interpreting it as a high concentration of quantum self-gravitating DM made of fermions of about 56 keV c^{-2} rest mass. This alternative approach can explain the astrometric data of both the S2-star and the G2 object with similar accuracy than the Schwarzschild BH scenario, but without introducing a drag force on G2 which is needed in the BH case to reconcile it with the G2 post-pericentre passage velocity data. An underlying assumption about the nature of such a DM quantum core is its absence of rotation, which is well supported by recent upper bounds on the spin of the central BH of $a < 0.1$, based on the spatial distribution of the S-stars (Ali et al. 2020; Fragione & Loeb 2020; Peißker et al. 2020). The first results obtained in Becerra-Vergara et al. (2020) within the DM scenario have been further extended in Becerra-Vergara et al. (2021) by considering the 17 best resolved stars orbiting Sgr A∗, achieving

★ E-mail: carguelles@fcaglp.unlp.edu.ar (CRA); eduar.becerra@icranet.org (EAB-V); jorge.rueda@icra.it (JAR)

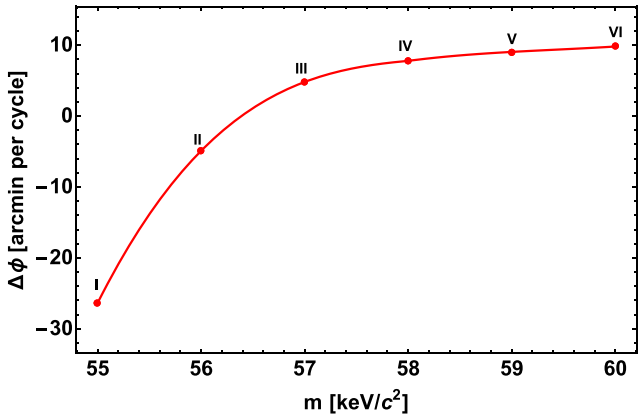

Figure 1. Relativistic periapsis precession $\Delta\phi$ per orbit as a function of the *darkino* mass as predicted by the RAR DM models for the S2-star. The precession is retrograde for $m < 56.4$ keV c^{-2} while it becomes prograde for $m > 56.4$ keV c^{-2} (see also Table 1).

an equally good fit than in the BH paradigm. Remarkably, such a dense DM core is the central region of a continuous distribution of DM whose diluted halo explains the Galactic rotation curves (Argüelles et al. 2018; Becerra-Vergara et al. 2020, 2021). Core-halo DM distributions of this kind are obtained from the solution of the Einstein equations for a self-gravitating, finite-temperature fluid of fermions in equilibrium following the Ruffini–Argüelles–Rueda (RAR) model (Ruffini, Argüelles & Rueda 2015; Argüelles et al. 2016, 2018, 2019, 2021; Gómez et al. 2016; Gómez & Rueda 2017; Becerra-Vergara et al. 2020, 2021; Penacchioni et al. 2020; Yunis et al. 2020). These novel core-halo DM profiles, as the ones applied in this Letter, have been shown to form and remain stable in cosmological time-scales, when accounting for the quantum nature of the particles within proper relaxation mechanisms of collisionless fermions (Argüelles et al. 2021). There are other alternative scenarios for Sgr A∗ involving a compact object of quantum nature, e.g. a boson star composed of ultralight scalars (see e.g. Torres et al. 2000). However, unlike the ∼50–345 keV c^{-2} fermionic DM RAR solutions, those boson stars do not explain the Galaxy rotation curves.

In this Letter, we focus the attention solely on the S2-star, which has been continuously monitored in the last 27 yr, and shows one of the most compact orbits around Sgr A∗ with an orbital period of about 16 yr and a pericentre of 0.56 Mpc (i.e. about 1450 Schwarzschild radii of the 4×10^6 M$_\odot$ central object). Even though it is relatively far from Sgr A∗ where relativistic effects are feeble and hard to detect, S2 is currently considered the best tracer of the Sgr A∗ gravitational potential. Being its most precise astrometric data taken around pericentre passages, see e.g. Gravity Collaboration et al. (2018a, 2020) and Do et al. (2019).

With the aim of making progress in disentangling the nature of Sgr A∗, we analyse here the relativistic periapsis precession of the S2-star in the above BH and DM scenarios. As the main result of this work, it is shown that the precession of the S2-star within the RAR DM model can be either retrograde or prograde depending on the amount of DM mass enclosed within the orbit. The latter is shown to be a function of the mass of the DM fermion (hereafter *darkino*). In particular, we show that for a 56 keV c^{-2} *darkino* mass, the RAR model predicts a retrograde S2 orbit precession, while for a slightly larger *darkino* mass of 58 keV c^{-2}, it predicts a prograde precession. The latter very much similar to the Schwarzschild BH case. By fitting all the publicly available S2 astrometric data, we conclude that none of the above scenarios about the nature of Sgr A∗ can be currently discriminated. This is mainly due to the large eccentricity of the S2 orbit, implying that its cumulative precession has a better chance of detectability away from the pericentre passage and closer to apocentre (Parsa et al. 2017). Consequently, we assess at which epoch during the S2 orbital motion these scenarios can be disentangled, being the S2 high precision data beyond 2019 of utmost importance for this task.

2 PRECESSION OF THE S2 ORBIT

In both models here considered for Sgr A∗, the spherically symmetric space–time metric can be written as $ds^2 = A(r)c^2dt^2 - B(r)dr^2 - r^2(d\theta^2 + \sin^2\theta d\phi^2)$, where (r, θ, ϕ) are the spherical coordinates, c is the speed of light, and $A(r)$, $B(r)$ are the metric functions to be found by solving the Einstein field equations. For the Schwarzschild BH model, such equations can be solved analytically leading to: $A(r) = 1 - 2GM_{\rm BH}/(c^2 r)$ and $B(r) = 1/A(r)$, where G is the gravitational constant and $M_{\rm BH}$ is the BH mass. For the RAR DM model, the system of Einstein equations is solved numerically for $A(r)$ and $B(r)$, together with the Tolman and Klein thermodynamic equilibrium conditions, and the (particle) energy conservation along geodesics (Argüelles et al. 2018). These metric potentials are not analytic and their radial dependence depend on the boundary-value problem specified to have solutions that agree with the galaxy observables. A solution of the RAR DM model for the case of the Milky Way, with specific boundary conditions that agree either with the overall rotation curve, the orbits of the 17 best resolved S-cluster stars, and the G2 object, was presented in Becerra-Vergara et al. (2020, 2021) for a *darkino* mass of 56 keV c^{-2}.

A necessary condition to be fulfilled by the RAR DM profiles in order to explain the S2 orbit, is that the corresponding DM core radius ($r_{\rm c}$) be smaller than the S2 pericentre (which for the case of $m = 56$ keV c^{-2} is $r_{\rm c} \approx 0.4$ Mpc $< r_{\rm p(S_2)} = 0.56$ Mpc). However, as first understood in Argüelles et al. (2018), and further detailed here, more compact DM cores with $r_{\rm c} < r_{\rm p(S_2)}$ (under fixed Milky Way halo boundary conditions) can also explain the S-cluster stellar orbits for different *darkino* masses. Thus, in this Letter, we explore other Milky Way RAR profiles from $m = 55$ to 60 keV c^{-2}, which will be essential to compare the properties of the S2 orbit precession for different central DM concentrations.

The equations of motion (e.o.m.) of a test particle in the above space–time metric, assuming without loss of generality the motion on the plane $\theta = \pi/2$, are $\dot{t} = E/(c^2 A(r))$; $\dot{\phi} = L/r^2$; $\ddot{r} = [-A'(r)\, c^2\, \dot{t}^2 - B'(r)\, \dot{r}^2 + 2\, r\, \dot{\phi}^2]/(2\, B(r))$, where E and L are, respectively, the conserved energy and the angular momentum of the test particle per unit mass, the overdot stands for derivative with respect to the proper time τ, while the superscript comma ($'$) denotes derivative with respect to the radial coordinate r. We perform the numerical integration of the e.o.m. with a Dormand–Prince algorithm (Strehmel 1988). In addition, the appropriate initial conditions have been chosen in such a way that the test particle motion starts at the apocentre, i.e. $t(\tau_0) = 0$, $\phi(\tau_0) = \pi$, $r(\tau_0) = r_{\rm a}$, and $\dot{r}(\tau_0) = 0$. We integrate the equations for a sufficiently long time, which assures that the particle performs more than two consecutive orbits, so we can compute the net precession of the real orbit over two consecutive cycles. For instance, denoting the time of apocentre in two consecutive orbits, respectively, as $t_{\rm apo1}$ and $t_{\rm apo2}$, the precession of the real orbit over those two cycles is $\Delta\phi = \phi(t_{\rm apo2}) - \phi(t_{\rm apo1})$.

We start by analysing the effects of different DM core concentrations with corresponding *darkino* masses, on the precession $\Delta\phi$ (as defined above) for the S2-star. For this task, we use all the publicly available astrometric measurements (Do et al. 2019) that include

Table 1. Comparison of the BH and RAR DM models that best fit of all the publicly available data of the S2 orbit.

	Model	$M_{\rm CO}$ [$10^6\,{\rm M}_\odot$]	$r_{\rm c}$ [Mpc]	$\Delta M_{\rm DM}/M_{\rm CO}$	$r_{\rm p}$ [as]	$r_{\rm a}$ [as]	$\langle\tilde{\chi}^2\rangle$	$\Delta\phi$ [arcmin]	$\Delta\phi_{\rm sky}$ [arcmin]
I	RAR ($m = 55\,{\rm keV\,c^{-2}}$)	3.55	0.446	1.39×10^{-2}	0.01417	0.23723	2.9719	−26.3845	−32.1116
II	RAR ($m = 56\,{\rm keV\,c^{-2}}$)	3.50	0.427	5.99×10^{-3}	0.01418	0.23618	3.0725	−4.9064	−5.9421
III	RAR ($m = 57\,{\rm keV\,c^{-2}}$)	3.50	0.407	2.21×10^{-3}	0.01417	0.23617	3.2766	4.8063	5.8236
IV	RAR ($m = 58\,{\rm keV\,c^{-2}}$)	3.50	0.389	7.13×10^{-4}	0.01424	0.23609	3.2814	7.7800	9.4243
V	RAR ($m = 59\,{\rm keV\,c^{-2}}$)	3.50	0.371	2.93×10^{-4}	0.01418	0.23613	3.3356	9.0456	10.9613
VI	RAR ($m = 60\,{\rm keV\,c^{-2}}$)	3.50	0.355	1.08×10^{-4}	0.01423	0.23610	3.3343	9.8052	11.8764
	BH	4.07	3.89×10^{-4}	0	0.01427	0.23623	3.3586	11.9501	14.4947

The second column shows the central object mass, $M_{\rm CO}$. For the Schwarzschild BH model, $M_{\rm CO} = M_{\rm BH}$, while for the RAR model, $M_{\rm CO} = M_{\rm c}$, with $M_{\rm c}$ the DM core mass. The third column shows the radius of the central object, $r_{\rm c}$. For the Schwarzschild BH model, $r_{\rm c}$ is given by the event horizon radius, $R_{\rm Sch} = 2GM_{\rm BH}/c^2$. The fourth column shows the DM mass enclosed within the S2 orbit, $\Delta M_{\rm DM}/M_{\rm CO}$. The best-fitting pericentre and apocentre radii of the S2 orbit are given, respectively, in the fifth and sixth columns. The values of the average reduced-χ^2 of the best fits, defined as in Becerra-Vergara et al. (2020), are given in the seventh column. The last two columns show, respectively, the model predictions of the periapsis precession of the real orbit, $\Delta\phi$, and of the sky-projected orbit, $\Delta\phi_{\rm sky}$.

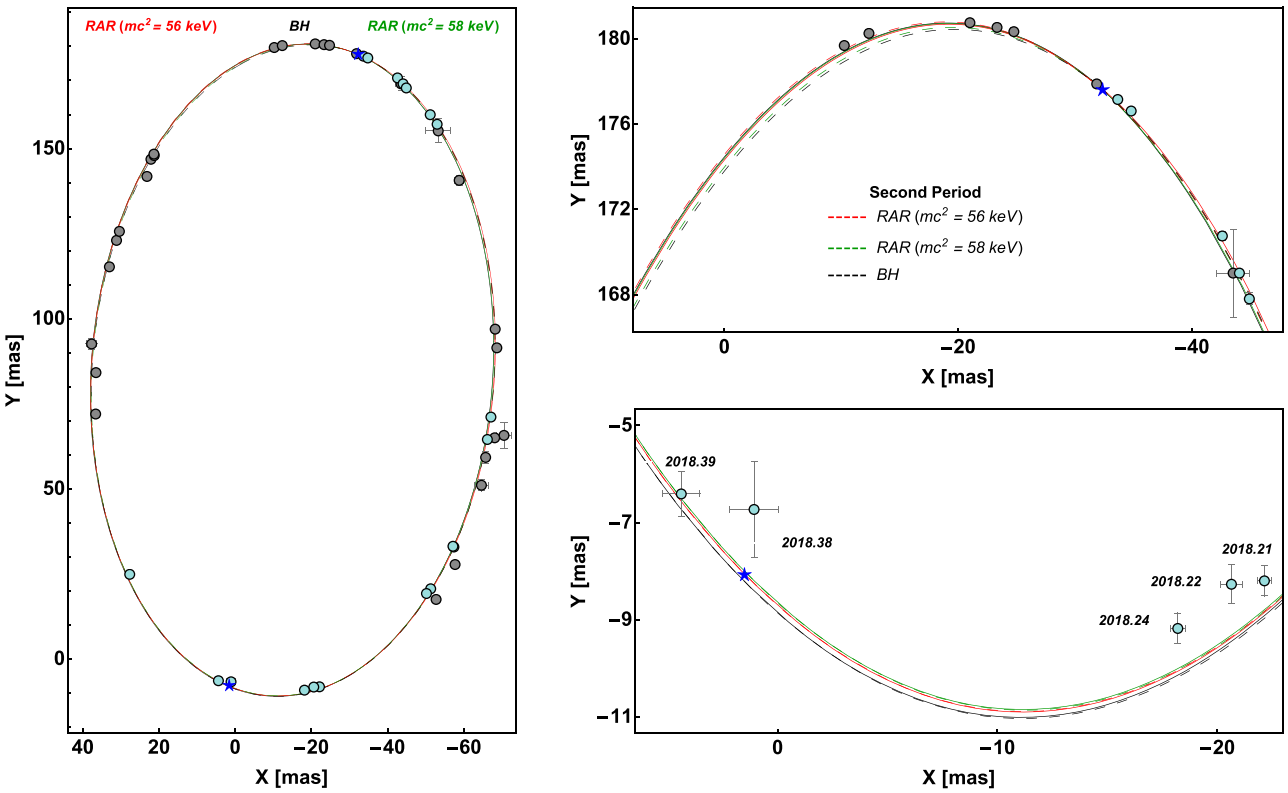

Figure 2. Relativistic precession of S2 in the projected orbit on the plane of the sky as predicted in the BH and RAR DM models. While it is prograde for the BH and RAR ($m = 58\,{\rm keV\,c^{-2}}$) (in dashed black and green, respectively), it is retrograde for the RAR DM model ($m = 56\,{\rm keV\,c^{-2}}$) (in dashed red). The solid (theoretical) curves and grey (data) points correspond to the first period (≈1994–2010) while the dashed (theoretical) curves and cyan (data) points to the second period (≈2010–2026). Right-hand panels: zoom of the region around apocentre (top panel) and pericentre (bottom panel). The astrometric measurements are taken from Do et al. (2019).

data obtained from the instruments NIRC on Keck I (1995–2005) and NIRC2 on Keck II (2005–2018). In Fig. 1, we show $\Delta\phi$ as a function of the *darkino* mass m, within a narrow particle mass range around $56\,{\rm keV\,c^{-2}}$. In the BH case, the precession of the orbit per cycle is given by the well-known expression $\Delta\phi_{\rm BH} = 6\pi GM_{\rm BH}/[c^2a(1-e^2)]$, which is always prograde ($\Delta\phi > 0$) and for a $4.07 \times 10^6\,{\rm M}_\odot$ BH mass and the S2 orbital parameters gives ≈12 arcmin. In the DM case, $\Delta\phi$ has no analytic expression, but the numerical solutions show that it increases non-linearly from negative to positive (i.e. from retrograde to prograde) with the *darkino* mass (see Fig. 1).

Given the DM quantum core is surrounded by an extended and more diluted DM mass, there are two competing effects in the RAR model which lead to three different possibilities for the S2 orbit precession. The effects can be roughly separated into a prograde effect caused by the gravitational potential of the DM core lying inside the S2 pericentre (similar to a relativistic point-like source), and a retrograde effect caused by the gravitational potential generated by the extended mass between the pericentre radius $r_{\rm p}$, and the apocentre radius $r_{\rm a}$, i.e. $\Delta M_{\rm DM} = \int_{r_{\rm p}}^{r_{\rm a}} 4\pi r^2 \rho_{\rm DM}(r){\rm d}r$. Due to the scaling behaviour of the core-halo RAR profiles with the underlying

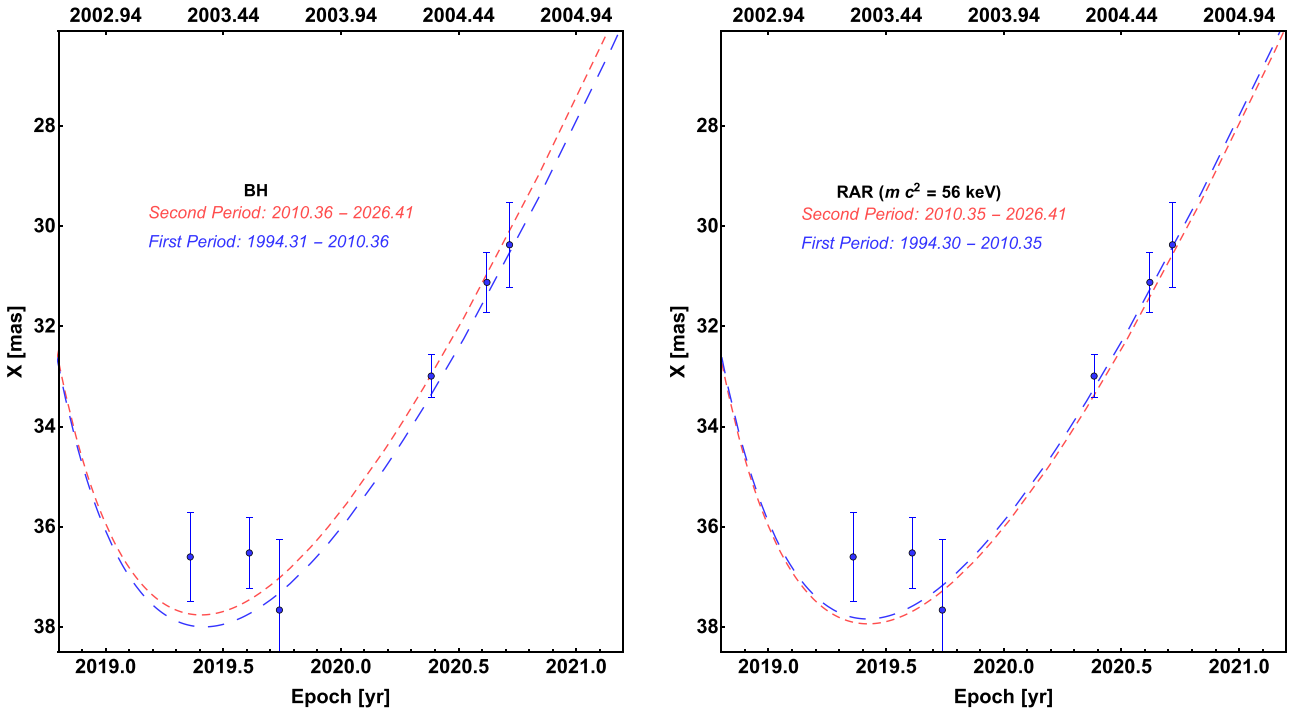

Figure 3. Relativistic precession of S2 as manifested in the right ascension as a function of time after last pericentre passage, where effects are more prominent. BH model (Left-hand panel) and RAR model for $m = 56$ keV c^{-2} (Right-hand panel).

four free parameters of the theory (Argüelles et al. 2018, 2019), both effects are related to each other. That is, the larger the *darkino* mass is, the more compact the DM core is (resembling more and more the BH case; Argüelles et al. 2018), with consequent less extended mass fraction $\Delta M_{\rm DM}/M_{\rm c}$. The above leads to: (i) Prograde precession ($\Delta\phi > 0$) as shown in Fig. 1 and occurring for $m > 56.4$ keV c^{-2} with a corresponding DM core mass of $M_{\rm c} = 3.50 \times 10^6\,{\rm M}_\odot$. In this case, the retrograde effect due to the extended DM mass $\Delta M_{\rm DM}/M_{\rm c}$ is not enough to compensate for the prograde one. For larger fermion masses, this prograde trend gets closer to the Schwarzschild value of 11.95 arcmin, and is approached for $m \approx 345$ keV c^{-2}, the mass value for which the DM core becomes unstable against gravitational collapse into a $\sim 4.2 \times 10^6\,{\rm M}_\odot$ BH (Argüelles et al. 2018). (ii) Null precession ($\Delta\phi = 0$) occurring for $m = 56.4$ keV c^{-2} with $M_{\rm c} = 3.50 \times 10^6\,{\rm M}_\odot$ when the above two effects balance each other. (iii) Retrograde precession ($\Delta\phi < 0$), as shown in Fig. 1 for $m < 56.4$ keV c^{-2} when the fraction of the DM core mass $\Delta M_{\rm DM}/M_{\rm c}$ between $r_{{\rm p}(S_2)}$ and $r_{{\rm a}(S_2)}$ is large enough. As detailed in Table 1, such a threshold value of $\Delta M_{\rm DM}/M_{\rm c}$ below which its associated retrograde effect becomes negligible (and thus the precession is always prograde) is ~ 0.1 per cent. Moreover, for $m > 57$ keV c^{-2}, the fraction of extended mass, $M_{\rm DM}/M_{\rm CO}$, falls below 0.1 per cent, in agreement with the current bounds for an extended mass within the S2 orbit in the Schwarzschild BH case (Gravity Collaboration et al. 2020).

Then, we proceed to compare the predictions on the periapsis precession of the S2-orbit analogous to that of Fig. 1, i.e. calculated at apocentre, but in the plane of the sky ($\Delta\phi_{\rm sky}$) for seven different models: one Schwarzschild BH and six RAR DM models for the Milky Way (i.e. already reproducing its rotation curve) with m from 55 and up to 60 keV c^{-2}. The obtained values of $\Delta\phi_{\rm sky}$ are given in the last column of Table 1, together with each set of free model parameters (e.g. $M_{\rm BH}$ for the BH model and $M_{\rm c}$ for RAR at each given m) that best fits the astrometry data of S2. Some a posteriori model properties including the DM core radius $r_{\rm c}$ and the extended DM mass fraction $\Delta M_{\rm DM}/M_{\rm c}$ are included in the table. The best-fitting models are obtained following the procedure of Becerra-Vergara et al. (2020), where the full set of best-fitting orbital parameters of S2 (for $m = 56$ keV c^{-2}) can also be found.

Fig. 2 shows the relativistic precession of S2 projected orbit, in a *right ascension–declination* plot. It can be there seen that while the positions in the plane of the sky nearly coincide about the last pericentre passage in the three models, they can be differentiated close to next apocentre. Specifically, the upper right-hand panel evidences the difference at apocentre between the prograde case (as for the BH and RAR model with $m = 58$ keV c^{-2}) and the retrograde case (i.e. RAR model with $m = 56$ keV c^{-2}).

The same conclusion can be better evidenced, and quantified, by showing the S2 orbit precession effects in right ascension (X) as a function of time, as predicted by each of the above two models. This is plotted in Fig. 3 showing the clear difference in X between two consecutive periods, each one starting at about the pericentre passage. The first period is shown by the long-dashed blue curve, and the second period is shown by the short-dashed red curve which extends beyond the last pericentre passage, where the predicted precession in each model is more evident. Indeed, the BH case (left-hand panel) shows a prograde trend with a maximal shift of $\Delta{\rm X} \approx 0.7$ mas at 2026.0 with respect to the former period (and being $\approx$0.4 mas at 2021.2), while the RAR ($m = 56$ keV c^{-2}) case (right-hand panel) shows a retrograde trend with a maximal shift of $\Delta{\rm X} \approx 0.3$ mas at 2026.3 with respect to the former period (being $\Delta{\rm X} \approx 0.2$ mas at 2021.2).

Unfortunately, the publicly available data in the relevant time-window of Fig. 3 are only a few data points within the first period [shown in blue dots and obtained from Do et al. (2019)], where the large error bars impede to discriminate between the models. Even if

the improved S2 astrometric resolution obtained by the GRAVITY Collaboration between 2018 and 2019.7 reaches the 0.1 mas, it covers the range around pericentre passage where the predicted ΔX in both models is too low to safely discriminate between these models.

3 DISCUSSION AND CONCLUSIONS

In this Letter, we have demonstrated that unlike the classical Schwarzschild BH prograde precession for the S2 orbit, when assuming a quantum DM nature for Sgr A$*$ according to the RAR model, it can be either retrograde or prograde depending on the amount of DM mass enclosed within the S2 orbit. Such a trend, in turn, depends on the *darkino* mass. We have shown that within the current astrometric resolution for S2, upcoming data close to the next apocentre passage have a good chance to validate one of the above predicted directions of the orbital precession. Additional constraints to the *darkino* mass could arise from the orbits of the faint stars S62 and S4714 whose pericenters have been estimated to be about one order of magnitude smaller than that of S2 (Peißker et al. 2020). If confirmed, the fermion mass would need to be larger ($\sim$100 keV c^{-2}) for the quantum core to be compact enough to lie inside those pericentre distance and produce such elliptic orbits.

Finally, we outline some astrophysical and cosmological consequences of the RAR DM model, in addition to the present results. The RAR model predicts a mechanism for supermassive BH formation in the high-redshift Universe when the dense core of DM reaches its critical mass for gravitational collapse (Argüelles et al. 2021). For a *darkino* mass of about 50 keV c^{-2}, such a critical mass is $\sim 10^8$ M$_\odot$. This numerical value can be affected by the additional accretion of baryonic matter on the *darkino* core. Furthermore, the RAR model provides as well the quantum nature and mass of the DM particles, and the morphology of the DM profiles on inner halo scales. As recently shown in Argüelles et al. (2021), the formation of *core–halo* RAR DM profiles is predicted within violent relaxation mechanisms with the following key properties. (i) They form and remain stable within cosmological time-scales. (ii) They are *universal*, ranging from the scales of dwarfs up to the galaxy cluster scales (Argüelles et al. 2019). (iii) On inner halo scales, the RAR density profiles develop an extended plateau (similar to Burkert profiles), thereby not suffering from the core-cusp problem associated with the standard Lambda cold dark matter cosmology (see e.g. Bullock & Boylan-Kolchin 2017).

ACKNOWLEDGEMENTS

CRA was supported by the Consejo Nacional de Investigaciones Científicas y Técnicas (CONICET) Argentina, Agencia Nacional de Promoción Científica y Tecnológica (grant PICT-2018-03743), and the International Center for Relativistic Astrophysics Network. EAB-V thanks financial support from COLCIENCIAS, ICRANet–IRAP-PhD, and Universidad Industrial de Santander (UIS).

DATA AVAILABILITY

The astrometric data used here were obtained from Do et al. (2019). The data generated here are available in Table 1.

REFERENCES

Ali B. et al., 2020, ApJ, 896, 100
Argüelles C. R., Mavromatos N. E., Rueda J. A., Ruffini R., 2016, J. Cosmol. Astropart. Phys., 2016, 038
Argüelles C. R., Krut A., Rueda J. A., Ruffini R., 2018, Phys. Dark Universe, 21, 82
Argüelles C. R., Krut A., Rueda J. A., Ruffini R., 2019, Phys. Dark Universe, 24, 100278
Argüelles C. R., Díaz M. I., Krut A., Yunis R., 2021, MNRAS, 502, 4227
Becerra-Vergara E. A., Argüelles C. R., Krut A., Rueda J. A., Ruffini R., 2020, A&A, 641, A34
Becerra-Vergara E. A., Argüelles C. R., Krut A., Rueda J. A., Ruffini R., 2021, MNRAS, 505, L64
Boehle A. et al., 2016, ApJ, 830, 17
Bullock J. S., Boylan-Kolchin M., 2017, ARA&A, 55, 343
Do T. et al., 2019, Science, 365, 664
Eckart A., Genzel R., 1997, MNRAS, 284, 576
Fragione G., Loeb A., 2020, ApJ, 901, L32
Genzel R., Eisenhauer F., Gillessen S., 2010, Rev. Mod. Phys., 82, 3121
Ghez A. M., Klein B. L., Morris M., Becklin E. E., 1998, ApJ, 509, 678
Ghez A. M., Salim S., Hornstein S. D., Tanner A., Lu J. R., Morris M., Becklin E. E., Duchêne G., 2005, ApJ, 620, 744
Ghez A. M. et al., 2008, ApJ, 689, 1044
Gillessen S., Eisenhauer F., Trippe S., Alexander T., Genzel R., Martins F., Ott T., 2009, ApJ, 692, 1075
Gillessen S. et al., 2017, ApJ, 837, 30
Gómez L. G., Rueda J. A., 2017, Phys. Rev., 96, 063001
Gómez L. G., Argüelles C. R., Perlick V., Rueda J. A., Ruffini R., 2016, Phys. Rev., 94, 123004
Gravity Collaboration et al., 2018a, A&A, 615, L15
Gravity Collaboration et al., 2018b, A&A, 618, L10
Gravity Collaboration et al., 2020, A&A, 636, L5
Matsumoto T., Chan C.-H., Piran T., 2020, MNRAS, 497, 2385
Parsa M., Eckart A., Shahzamanian B., Karas V., Zajacek M., Zensus J. A., Straubmeier C., 2017, ApJ, 845, 22
Peißker F., Eckart A., Zajacek M., Ali B., Parsa M., 2020, ApJ, 899, 50
Penacchioni A. V., Civitarese O., Argüelles C. R., 2020, Eur. Phys. J., 80, 183
Ruffini R., Argüelles C. R., Rueda J. A., 2015, MNRAS, 451, 622
Schödel R. et al., 2002, Nature, 419, 694
Strehmel K., 1988, J. Appl. Math. Mech., 68, 260
Torres D. F., Capozziello S., Lambiase G., 2000, Phys. Rev., 62, 104012
Tursunov A., Zajacek M., Eckart A., Kološ M., Britzen S., Stuchlík Z., Czerny B., Karas V., 2020, ApJ, 897, 99
Yunis R., Argüelles C. R., Mavromatos N. E., Moliné A., Krut A., Carinci M., Rueda J. A., Ruffini R., 2020, Phys. Dark Universe, 30, 100699

This paper has been typeset from a TEX/LATEX file prepared by the author.